An Integrated Finite Difference Method for Analyzing Fluid Flow in Porous Media

T. N. NARASIMHAN

Department of Civil Engineering, University of California, Berkeley, California 94720

P. A. WITHERSPOON

Lawrence Berkeley Laboratory, University of California, Berkeley, California 94720

The theoretical basis for the integrated finite difference method (IFDM) is presented to describe a powerful numerical technique for solving problems of groundwater flow in porous media. The method combines the advantages of an integral formulation with the simplicity of finite difference gradients and is very convenient for handling multidimensional heterogeneous systems composed of isotropic materials. Three illustrative problems are solved to demonstrate that two- and three-dimensional problems are handled with equal ease. Comparison of IFDM with the well-known finite element method (FEM) indicates that both are conceptually similar and differ mainly in the procedure adopted for measuring spatial gradients. The IFDM includes a simple criterion for local stability and an efficient explicit-implicit iterative scheme for marching in the time domain. If such a scheme can be incorporated in a new version of FEM, it should be possible to develop an improved numerical technique that combines the inherent advantages of both methods.

INTRODUCTION

Numerical analysis of fluid flow through porous media in problems with complex geometry is greatly facilitated by the use of integral formulations. Perhaps the most widely used integral method is the finite element method (FEM), which can be based on variational principles or the Galerkin approach.

In this paper we will describe another integral formulation which has been successfully used to solve heat transfer problems in heterogeneous isotropic multidimensional flow regions. For reasons that will become clear later, we shall call this method the 'integrated finite difference method' (IFDM). Although the method has been used in studying groundwater systems [*Todd*, 1959; *Tyson and Weber*, 1964; *Cooley*, 1971], it does not appear to have been widely employed in the field of hydrogeology. It is our opinion, however, that the IFDM can be a very powerful tool in analyzing heterogeneous groundwater systems with complex geometries. Furthermore, in comparing the conceptual bases of IFDM and FEM we find that they have much in common.

The purpose of this paper is first to develop the IFDM equations and demonstrate the power of the method with three different problems. We will then examine the conceptual bases of both IFDM and FEM and attempt to identify those features which give each of these techniques unique advantages in handling specific classes of problems. Finally, we will consider the possibility of developing a new technique which could combine some of the unique advantages of each method.

INTEGRATED FINITE DIFFERENCE METHOD

MacNeal [1953] is apparently the first worker to use the IFDM approach, and he classified it as an 'asymmetric finite difference network.' He used this approach in solving second-order boundary value problems. Subsequently, the method has been used successfully for solving heat transfer problems, and a good description of the approach and related aspects can be found in *Dusinberre* [1961]. *Edwards* [1972] used the IFDM in developing a powerful computer code called Trump for calculating transient and steady state temperature distributions in multidimensional systems, and the following discussion will be based in large measure on the Trump program. Although Trump can handle conductive, convective, and radiative heat transfer, we will restrict our attention to the heat conduction part of the program, since conductive heat transfer is conceptually similar to fluid flow in porous media.

Consider the partial differential equation for groundwater flow

$$\text{div } K \,\mathbf{grad}\, \phi + g = c\, \partial\phi/\partial t \tag{1}$$

For the sake of simplicity, we shall assume K and c in (1) to be constant and independent of ϕ, so that (1) is a linear equation.

We can spatially integrate (1) over a conveniently small finite subregion V of the flow region and write [*Encyclopedia of Science and Technology*, 1960]

$$\int_V (\text{div } K \,\mathbf{grad}\, \phi + g)\, dV = \frac{\partial}{\partial t} \int_V c\phi \, dV \tag{2}$$

We now use the divergence theorem to convert the first term on the left-hand side to a surface integral, and on the right-hand side we assume that c and ϕ are average values over V. Then

$$\int_S K \,\mathbf{grad}\, \phi \cdot \mathbf{n}\, dS + gV = cV \frac{\partial \phi}{\partial t} \tag{3}$$

The central concept of IFDM is to discretize the total flow domain into conveniently small subdomains or 'elements' and evaluate the mass balance in each element as indicated in (3). Physically, the surface integral on the left-hand side of (3) is the summation of fluxes over the surface S and thus measures the rate at which mass is accumulating in the element, as governed by initial and boundary conditions. The right-hand side converts the rate of accumulation of fluid into the corresponding average time rate of change in potential over the element.

To illustrate the IFDM, let the shaded region in Figure 1 be an element whose average properties are associated with a representative nodal point $m = 6$, which may be located anywhere within or on the boundaries of the element. For maximum accuracy, interfaces between elements should be perpendicular to the line joining the two nodal points and intersect that line at an appropriate mean position (arithmetic mean of nondivergent coordinates, log mean of cylindrical radii, or geometric mean of spherical radii). This ideal situation may be difficult to achieve in practice but should be approximated as closely as possible [*Edwards*, 1972]. In Figure 1, element m is connected to adjoining elements $n = 1$–5. Under these conditions the finite difference approximation for (3) can be written

$$g_m V_m + \sum_n \bar{K}_{m,n} \frac{\phi_n - \phi_m}{D_{m,n}} A_{m,n} = c_m V_m \frac{\Delta\phi_m}{\Delta t} \qquad (4)$$

where $\bar{K}_{m,n}$ is the harmonic mean permeability when elements m and n are composed of different materials.

For appropriately small values of Δt, (4) can be written in a stable explicit form as

$$\frac{\Delta t}{c_m V_m} [g_m V_m + \sum_n U_{m,n}(\phi_n^0 - \phi_m^0)] = \Delta\phi_m \qquad (5)$$

Here, $U_{m,n} = (\bar{K}_{m,n} A_{m,n})/D_{m,n}$ is the 'conductance' of the interface-separating elements m and n and represents the rate of fluid transfer per unit difference in potential between nodal points m and n. The terms ϕ_m^0 and ϕ_n^0 represent the initial values of potentials at the beginning of the interval Δt. Equation (5) can be directly used to solve for $\Delta\phi_m$ if the geometric parameters $A_{m,n}$, $D_{m,n}$, and V_m are provided as input data, in addition to the material properties K and c.

If it is desired to use large values of Δt, then (4) can be expressed implicitly as

$$\frac{\Delta t}{c_m V_m} \{g_m V_m + \sum_n U_{m,n}[(\phi_n^0 + \lambda\Delta\phi_n) - (\phi_m^0 + \lambda\Delta\phi_m)]\} = \Delta\phi_m \qquad (6)$$

where $0 < \lambda < 1$. When $\lambda = 0$, (6) reduces to the forward-differencing scheme (5). When $\lambda = 1$, (6) becomes a fully implicit backward-differencing scheme, while $\lambda = \frac{1}{2}$ yields the well-known central-differencing, or Crank-Nicholson, procedure. For unconditional stability, $\lambda > \frac{1}{2}$. Both prescribed potential and prescribed flux boundaries or even mixed boundary conditions can be suitably handled as described by *Edwards* [1972] and *Narasimhan* [1975].

It can be shown either from simple reasoning [*Dusinberre*, 1961] or on the basis of an analysis of error propagation [*O'Brien et al.*, 1951; *Evans et al.*, 1954; *Narasimhan*, 1975] that for each element m, there is a critical time constant Δt_m such that (5) is unstable if $\Delta t > \Delta t_m$. The magnitude of this critical time constant is given by

$$\Delta t_m = c_m V_m / \sum_n U_{m,n} \qquad (7)$$

where n now stands for all elements connected to element m. Physically, Δt_m represents the approximate time required for element m to react significantly to changes in potential in the adjacent elements to which m is connected [*Edwards*, 1972]. Obviously, if $\Delta t > \Delta t_m$ for any element m, one would have to use (6) instead of (5) for that particular element with $\frac{1}{2} \leq \lambda \leq 1$.

The implicit calculations inherent in the application of (6) can be carried out either with the help of matrix inversion techniques or with the help of iterative techniques. The Trump computer program [*Edwards*, 1972] employs an iterative technique based on the generalization of a method suggested by *Evans et al.* [1954]. Using this approach and recognizing the fact that the critical time step Δt_m is defined for each element, *Edwards* [1972] has successfully incorporated in Trump a technique by which explicit calculations are carried out for those elements where $\Delta t < \Delta t_m$ and implicit calculations for the balance where $\Delta t > \Delta t_m$, with $\frac{1}{2} \leq \lambda \leq 1$. When the IFDM is combined with the explicit-implicit iterative scheme developed in Trump, it provides a very useful tool in analyzing fluid flow problems in heterogeneous systems.

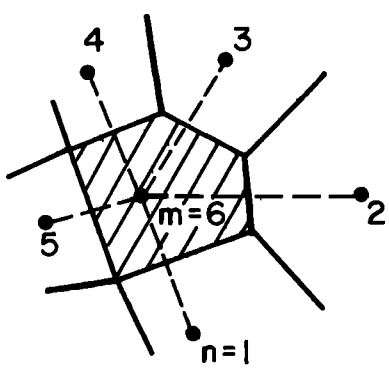

Fig. 1. An element with its representative nodal point in the IFDM network.

Solutions to Illustrative Problems

To illustrate the utility of the IFDM, we shall consider three problems for which analytical solutions are available. The first of these has been chosen to demonstrate the accuracy that can be expected from IFDM. The second is designed to demonstrate the ability of IFDM to solve three-dimensional problems. The last example serves to illustrate the use of the method in approaching systems with radially symmetric geometry, in which the material distribution can be asymmetric.

Theis problem. A classical problem in the field of groundwater hydrology is that of nonsteady radial flow to a well discharging at a constant rate Q and piercing a horizontally infinite homogeneous and isotropic aquifer. The solution to this problem is the well-known *Theis* [1935] equation

$$s = \frac{Q}{4\pi T} \int_{r^2 S/4Tt}^{\infty} \frac{e^{-u}}{u} du \qquad (8)$$

Pinder and Frind [1972] have shown how the FEM developed from the Galerkin formulation can be used to simulate the Theis solution. They verified the accuracy of their FEM results in comparison with the analytical solution using linear as well as isoparametric elements. Their FEM mesh consisted of only nine nodal points along any radial line from the well. To check the accuracy of IFDM, we set up a mesh with nine nodal points along a radial line such that the distances from the origin were identical to those of *Pinder and Frind* [1972]. They report their results for the node at $r = 12.7$ feet as shown in Figure 2, but they do not indicate the magnitude of the time steps used in obtaining these results. We solved the same problem, using IFDM and the mixed explicit-implicit scheme of *Edwards* [1972] with time steps that varied from an initial value of $\Delta t = 3.6 \times 10^{-3}$ s to a maximum value of $\Delta t = 5000$ s in reaching a total time of 10^5 s. In Figure 2 we give our results at $r = 12.7$ feet. It can be seen that over the time period

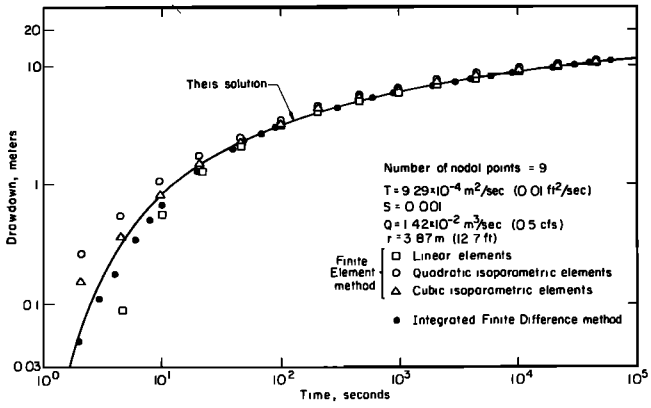

Fig. 2. A comparison of numerical results with the analytical solution for the Theis problem.

studied, the IFDM results compare very favorably with the analytical solution.

Continuous point source problem. An advantage of formulating the governing equation in the form of (5) or (6) is that these equations are equally valid in one, two, or three dimensions. Therefore the IFDM can handle one-, two-, or three-dimensional problems with equal ease. To verify the ability of IFDM to handle three-dimensional flow, we applied the method to the problem of a continuous point source in an isotropic medium. The analytical solution is given by *Carslaw and Jaeger* [1959] as

$$\phi(r, t) - \phi_0(r, t_0) = \frac{Q}{4\pi\kappa r} \operatorname{erfc}\left[\frac{r}{(4\kappa t)^{1/2}}\right] \qquad (9)$$

To solve the above problem in three dimensions by using the IFDM, the flow region was visualized as a sphere enclosed in a cube. Thus the spherical elements near the point source gradually lost their curvature in grading outward to cubic-shaped elements at the outer boundary (Figure 3). This was done so that one could accurately simulate spherical symmetry close to the source and at the same time allow for more general conditions of flow near the outer limits. The flow region was everywhere subdivided into three-dimensional elements. From considerations of symmetry (eight octants in a cube and three Cartesian axes) a wedge-shaped portion of the flow region, whose volume is 1/24 of a cube, was chosen for actual modeling, as is illustrated in Figure 3.

The shortest distance from the point source to the outer boundary of the wedge was 400 m. The mesh consisted of 47 three-dimensional elements and 87 interfaces between elements. Owing to the curvilinear nature of the elements, different nodal points were located along different radial lines from the point source. Distances from the source to nodal points varied from 1 m for the closest to 593 m for the farthest, while element volumes ranged from 9.1×10^{-1} to 1.09×10^{6} m³. The problem was solved with the following arbitrary parameters: $Q = 10^{3}$ m³/s, $K = 10^{-3}$ m/s, and $c = 10^{-2}$ m^{-1}. Impermeable conditions were assumed on all faces of the wedge-shaped flow region.

The results of the computations are shown in Figure 4. Instead of presenting the data in dimensionless form we can demonstrate the overall accuracy in more detail by plotting drawdown as a function of time for various distances (Figure 4*a*) and drawdown as a function of distance for various times (Figure 4*b*) in comparison to the analytical solution. The problem was solved from 0 to 10^{6} s in 683 time cycles by using

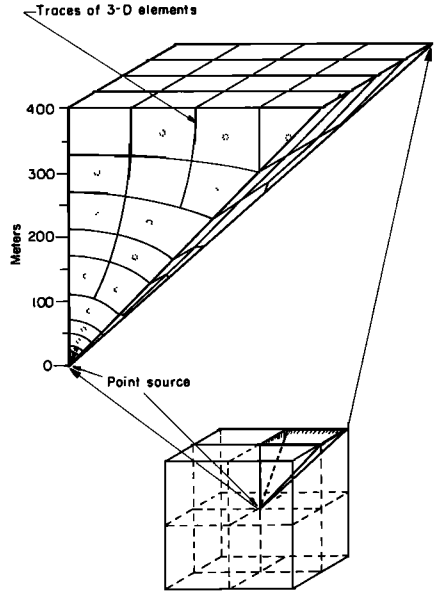

Fig. 3. A three-dimensional IFDM network of elements for the point source problem.

the mixed explicit-implicit scheme. The magnitude of the time steps varied from 1×10^{-1} to 8.5×10^{8} s. The simulation took 8.5 s of CDC 7600 machine time.

Figures 4*a* and 4*b* show that the computed results deviate from the analytical solution for small values of time and at small radial distances. However, we believe that the overall agreement with the analytical solution is quite good, and we conclude that the IFDM has successfully been used in solving this three-dimensional problem.

Fracture flow problem. The parallel plate formulation for flow in a fracture is widely used by many workers [*Snow*, 1965; *Romm*, 1966; *Louis*, 1969; *Sharp and Maini*, 1972; *Wilson and Witherspoon*, 1974; *Gale et al.*, 1974] and leads to a fracture permeability defined as

$$k = \rho g b^2/12\mu \qquad (10)$$

However, when the fracture closes, the surfaces do not neces-

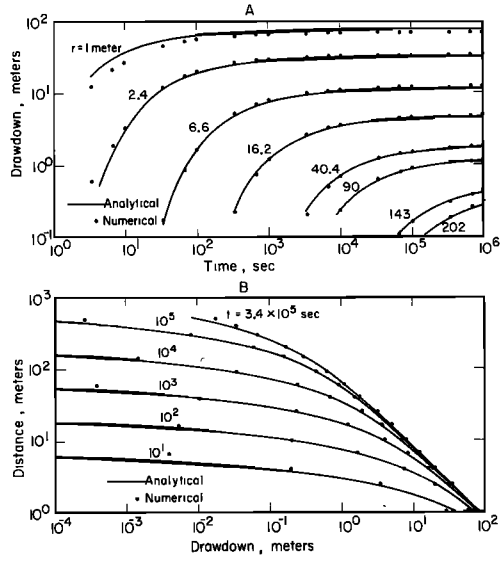

Fig. 4. A comparison of the numerical results with the analytical solution for the point source problem: (*a*) time drawdown and (*b*) distance drawdown.

sarily touch at every point, and this becomes quite obvious when any natural fracture is examined in detail. This has led some investigators [*Louis*, 1969; *Sharp and Maini*, 1972] to suggest that the exponent in (10) is some value less than 2 for a fracture that is being closed under normal stress.

In other work in this laboratory we are currently investigating this problem using a single horizontal fracture under conditions of radial flow. The fracture is formed by two cylindrical blocks of impermeable rock, 0.152 m in diameter, each having smooth faces. Flow originates at a 0.0254-m-diameter hole in the center that is concentric with the external boundary. If the circular fracture is open and the planar surfaces are parallel, then the steady state flow is given by

$$Q = (2\pi\rho g b^3 \Delta\phi)/[12\mu \ln (r_e/r_i)] \qquad (11)$$

To investigate this problem, we have used the IFDM and set up a flow net of elements as shown in Figure 5. The flow region has been discretized into 264 elements with 456 interfaces, and permeability within each element is given by (10).

As a practical problem of interest in the laboratory work we solved an arbitrary case where $\Delta\phi = 21.09$ m of water (30 psi), $\rho = 1000$ kg/m^3, $\mu = 0.001$ kg/m s, and $b = 1.27 \times 10^{-4}$ m. From (11) one can quickly compute

$$Q = \frac{2\pi(1000)(9.8)(1.27 \times 10^{-4})^3(21.09)}{12(0.001) \ln (0.076/0.0127)}$$

$$= 1.237 \times 10^{-4} \text{ m}^3/\text{s}$$

We then solved the same problem, using IFDM and the network shown in Figure 5 and obtained $Q = 1.227 \times 10^{-4}$ m^3/s. Pressures should be a linear function of ln r, and a comparison of IFDM results with those from the analytical solution is shown in Figure 6. The agreement is very good.

Of considerably more interest is the case where the fracture partially closes and the areas of contact are impermeable. This kind of heterogeneity can be handled with the IFDM by assuming that certain elements within the network of Figure 5 have zero permeability. The results of a hypothetical problem with a random distribution of impermeable elements are given in Figure 7. Here the pressure head has been normalized in terms of percent of the injection pressure. The pressure profile along line AB of Figure 7 is shown in Figure 6. For the same aperture and flow conditions as were given above, the flow was

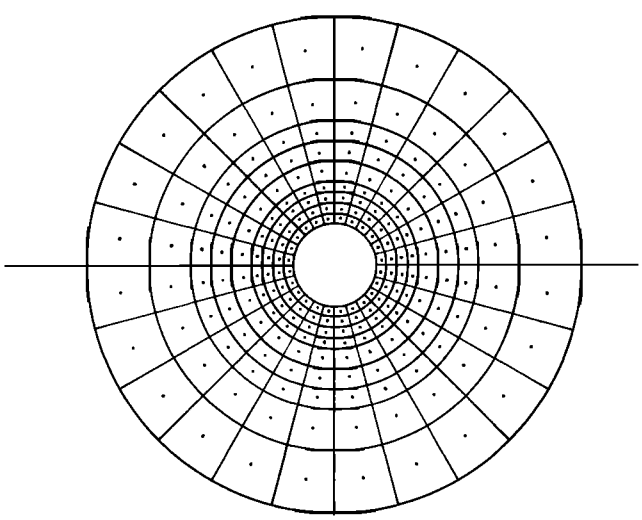

Fig. 5. A two-dimensional IFDM network of elements for the fracture flow problem.

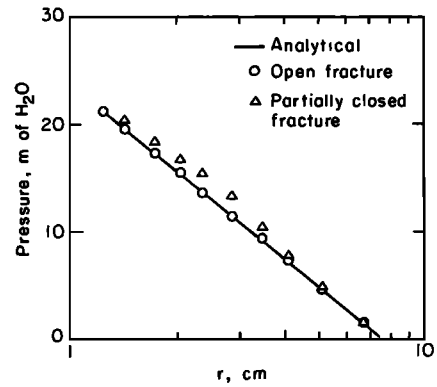

Fig. 6. A comparison of the numerical results with the analytical solution for the fracture flow problem.

found to be 8.032×10^{-5} m^3/s. In other words, the impermeable contact area that amounts to about 15% of the total fracture surface caused a reduction in flow of approximately 35%. Computer simulations of carefully chosen hypothetical situations for this kind of fracture flow can provide valuable assistance in analyzing laboratory data.

COMPARISON OF IFDM AND FEM

From the above discussion we have seen how the IFDM can be used to analyze transient fluid flow problems in multidimensional systems with complex geometry. The FEM is also well suited to such problems, and the question will arise as to how the two methods compare. A detailed analysis is not an easy task, and only a comparison of the overall features will be attempted here. Our purpose is to provide some clues for choosing an approach to certain classes of problems and also to provide an insight into the development of new techniques of analysis that will combine the inherent advantages of both IFDM and FEM.

Although FEM equations can be developed from variational principles [*Javandel and Witherspoon*, 1968] or physical considerations [*Winslow*, 1966; *Wilson*, 1968], mathematically, the most direct method is the Galerkin approach [*Zienkiewicz*

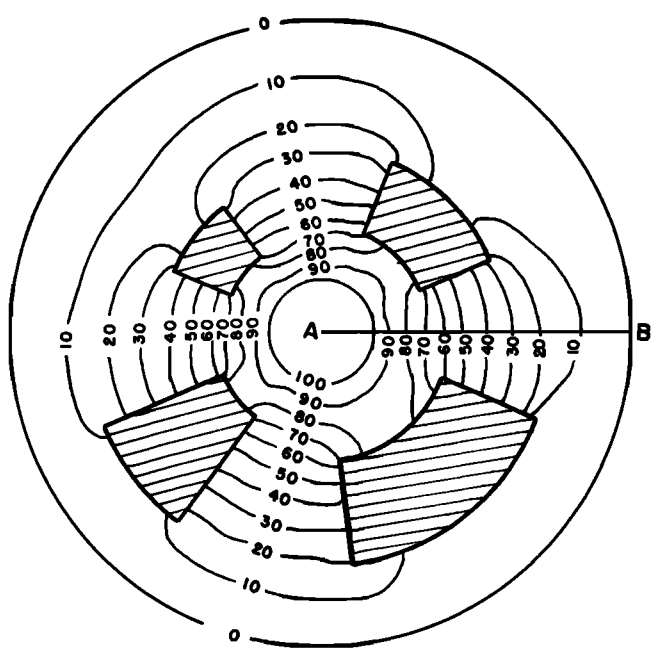

Fig. 7. The pressure distribution in a partially closed fracture.

and Parekh, 1970; *Pinder and Frind,* 1972; *Neuman,* 1973, 1975]. In the following we will analyze the Galerkin formulation of the FEM, and since the IFDM uses a linear approximation for potential gradient, we will restrict our analysis of FEM to triangular elements where a linear approximation is used.

In the Galerkin scheme the partial differential equation is first weighted with an appropriate weighting function and then integrated. Thus after neglecting the source term in (2), we have

$$\int_V \xi_m \left(\nabla \cdot K \nabla \xi_n \phi_n - c \frac{\partial \xi_n \phi_n}{\partial t} \right) dV = 0 \qquad (12)$$

In writing (12) we have replaced ϕ by the approximate relation $\phi \approx \xi_n \phi_n$, where the repetition of n denotes summation over n nodal points. The particular feature of the Galerkin procedure is that the weighting function $\xi_m(x_i)$ is the same as the coordinate function $\xi_n(x_i)$ that is used to approximate ϕ. In the FEM, which is a subdomain scheme, ξ_m is defined as unity at nodal point m and zero at all other nodal points.

In the simplest case involving linear elements the FEM flow region is discretized into a series of appropriately small triangles, within each of which ϕ is assumed to vary linearly. Thus ξ_m also varies linearly from a value of 1 at nodal point m to zero along the line connecting the remaining two nodal points of the triangular element. For isotropic media, K in (12) is a scalar, and for anisotropic media, K is a second-rank symmetrical tensor.

Assuming K and c to be constant within each triangular element and making use of Green's first identity [*Sokolnikoff and Redheffer,* 1966], we can rewrite (12) as

$$\sum_{\text{all } e} \left(-\int_{V^e} \nabla \xi_m \cdot K \nabla \xi_n \phi_n \, dV + \int_{S^e} \xi_m K \nabla \xi_n \phi_n \cdot \mathbf{n} \, dS - \int_{V^e} \xi_m c \frac{\partial \xi_n \phi_n}{\partial t} \, dV \right) = 0 \qquad (13)$$

In (13) the superscript e denotes a triangular element, and the summation denotes integration over all elements of the flow region. One equation such as (13) is set up for each nodal point m at which the time rate of change of potential is to be determined. Furthermore, the nature of the weighting function ξ_m is such that the surface integral is zero for all interior nodal points. If m lies on a boundary of the flow region where the flux is prescribed, the surface integral becomes a known quantity.

Hence we need to concern ourselves only with the two volume integrals in (13). Moreover, by definition, ξ_m has nonzero values only in those elements that include nodal point m. Thus the summation implied in (13) actually means summation only over those triangular elements at whose apex m lies. We shall call the subdomain composed of these triangles the 'primary' element of m, while each triangular element will be called a 'secondary' element (Figure 8).

Let us now consider the first volume integral in (13) as applied to secondary element II in Figure 8. It can be shown [*Narasimhan,* 1975] that the integral $\int \nabla \xi_m \cdot K \nabla \xi_n \phi_n \, dV$, evaluated with respect to nodal point m, is simply the flux normal to the line connecting the midpoints A and B of the sides adjacent to m, as is shown in Figure 9. Furthermore, if G is the centroid of secondary element II, then because of the constant gradient of ϕ within the element the flux across the line AB is exactly equal to the flux across the line AGB. Hence extending this approach to all secondary elements shown in Figure 8 leads to the conclusion that $\sum_e \int \nabla \xi_m \cdot K \nabla \xi_n \phi_n \, dV$ is a summation of fluxes across the surface enclosing the subregion around nodal point m, as is shown in Figure 10.

Comparison of Figures 10 and 1 shows that the weighted integration of the spatial integral in the Galerkin scheme and the evaluation of the surface integral in the IFDM both lead to a summation of fluxes across the surface of a subdomain associated exclusively with the nodal point of interest. This summation can therefore be interpreted as the net rate at which fluid is accumulating within the exclusive subdomain associated with nodal point m.

The other volume integral in (13), $\int \xi_m c \, \partial \xi_n \phi_n / \partial t \, dV$, determines how the fluid accumulating in the exclusive subdomain of nodal point m (Figure 10) is distributed within the subdomain so as to cause ϕ_m to change with time. We will consider two possible ways of interpreting this integral.

First, let us review the conventional Galerkin procedure (12) in which $\xi_n \phi_n$ ($\approx \phi$) is substituted for ϕ in the time derivative. Assuming that c is constant within e and recognizing that $\xi_m(x_i)$ is independent of time, we get

$$\sum_e \int_{V^e} \xi_m c \frac{\partial \xi_n \phi_n}{\partial t} \, dV = \sum_e c^e \int_{V^e} \xi_m \xi_n \frac{\partial \phi_n}{\partial t} \, dV \qquad (14)$$

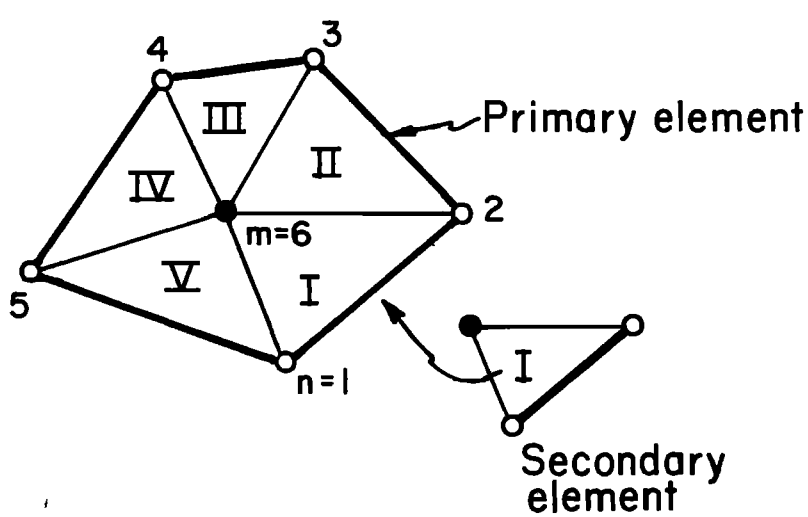

Fig. 8. Primary and secondary elements of a FEM network.

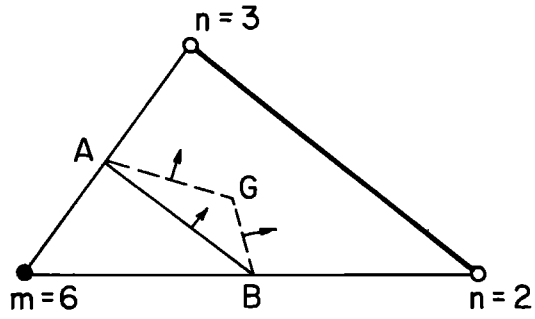

Fig. 9. An expanded view of secondary element II in Figure 8.

Using *Felippa*'s [1966] evaluation of $\int_{V^e} \xi_m \xi_n \, dV$ for triangular elements, we can rewrite (14) as

$$\sum_e \int_{V^e} \xi_m c \frac{\partial \xi_n \phi_n}{\partial t} \, dV = \sum_e c^e \left[\frac{\Delta^e}{6} \frac{\partial \phi_m}{\partial t} + \frac{\Delta^e}{12} \left(\frac{\partial \phi_n^{\,1}}{\partial t} + \frac{\partial \phi_n^{\,2}}{\partial t} \right) \right] \quad (15)$$

where $\partial \phi_n^{\,1}/\partial t$ and $\partial \phi_n^{\,2}/\partial t$ are time derivatives at the remaining two nodal points of element e. If we recognize that the exclusive subdomain associated with nodal point m in Figure 10 is one third of the area of the entire pentagon, (15) may be taken to imply that $\partial \phi_m/\partial t$, which is an average value representative of one sixth of the area of the pentagon, can be interpreted as the mean rate of change in potential over one half of the shaded subregion in Figure 10. Over the remaining half of this subregion the accumulating fluid is assumed to be distributed in accordance with the average time rates $\partial \phi_n/\partial t$ at the neighboring nodal points of m.

The second way to interpret the integral $\int_{V^e} \xi_m c \, \partial \xi_n \phi_n / \partial t \, dV$ is to consider that the net rate of fluid accumulation arising out of the first volume integral in (13) is distributed in such a fashion within the shaded subregion in Figure 10 that the time rate of change in potential is uniform throughout the exclusive subdomain. This would imply that in the second volume integral in (13) we should replace $\partial \xi_n \phi_n/\partial t$ by $\partial \phi^M/\partial t$, which is now the mean rate of change in potential over the exclusive subdomain of nodal point m. According to this interpretation we get instead of (15)

$$\sum_e \int_{V^e} \xi_m c \frac{\partial \phi^M}{\partial t} \, dV = \frac{\partial \phi^M}{\partial t} \sum_e c^e \int_{V^e} \xi_m \, dV = \frac{\partial \phi^M}{\partial t} \sum_e \frac{\Delta^e c^e}{3} \quad (16)$$

The right-hand side of (15) leads to a nondiagonal capacity matrix, while the right-hand side of (16) leads to a diagonal form. In attempting to extend the conventional Galerkin approach in (15) to the quasi-linear problem of unsaturated-saturated groundwater flow, *Neuman* [1973, 1975] found that he could not get a convergent solution unless he diagonalized the capacity matrix as was done in (16). He reasoned that since the Galerkin approximation applies only at a given instant of time, the time derivative in the governing equation should be determined independently of the orthogonalization process. *Emery and Carson* [1971] also indicate a preference for an FEM approach in which the time derivative is treated as it is in (16) rather than as it is in (15). Equation (16) also conforms to the purely physical development of the FEM equations of *Winslow* [1966] and *Wilson* [1968]. It may be noted here that the nondiagonal capacity matrix of (15) leads to an algorithm requiring both a larger computer storage requirement and a larger number of computational operations than the algorithm derived from the diagonal capacity matrix resulting from (16).

In summary, when m is an interior nodal point, the surface integral in (13) disappears, and depending on the choice of (15) or (16) the FEM equations can be written in either of the following two forms:

The conventional Galerkin form

$$-\sum_e \int_{V^e} \nabla \xi_m \cdot K \nabla \xi_n \phi_n \, dV = \sum_e c^e \left[\frac{\Delta^e}{6} \frac{\partial \phi_m}{\partial t} + \frac{\Delta^e}{12} \left(\frac{\partial \phi_n^{\,1}}{\partial t} + \frac{\partial \phi_n^{\,2}}{\partial t} \right) \right] \quad (17)$$

The modified Galerkin form

$$-\sum_e \int_{V^e} \nabla \xi_m \cdot K \nabla \xi_n \phi_n \, dV = \frac{\partial \phi^M}{\partial t} \sum_e \frac{\Delta^e c^e}{3} \quad (18)$$

Comparison of (18) with (5) or (6) shows that the modified Galerkin form is similar to the IFDM except for the difference in the procedure used for evaluating the gradient of ϕ. Comparison of (17) with (5) or (6) shows that the conventional Galerkin procedure is conceptually similar to IFDM in associating an exclusive subdomain with each nodal point of interest and summing the surface fluxes to evaluate the effect of the rate of fluid accumulation within the subdomain.

The interesting fact that emerges out of a comparison of IFDM with FEM is that the chief difference between the two methods lies in the manner in which the spatial gradients in ϕ are evaluated. The IFDM employs the simple finite difference approximation and is thus constrained to a measurement of gradients normal to a given surface and restricted to first-order approximations. As a result it cannot handle general tensorial quantities, since they require evaluation of tangential gradients along the reference surface in addition to the normal gradient. Moreover, when the spatial variation of ϕ is rapid, the IFDM would require a large number of mesh points to simulate accurately the rapid variation of ϕ in terms of successive linear segments.

The FEM, on the other hand, by setting up a surface $\phi = \xi_n \phi_n$ for the variation of potential over an elemental region, achieves a very general and powerful form of expressing the spatial variation of ϕ. As a result, the FEM is not only well suited for handling general tensorial parameters (e.g., stress, permeability, dispersion) but is also well suited to the utilization of higher-order surfaces, which can approximate the rapid spatial variation of ϕ with greater accuracy.

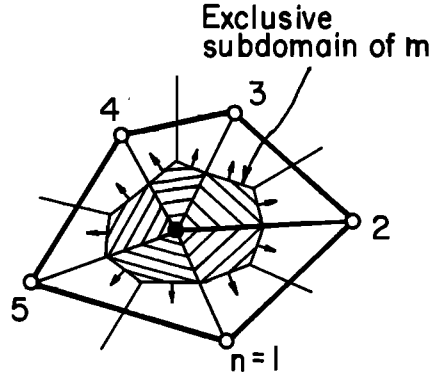

Fig. 10. An evaluation of the Galerkin spatial integral for nodal point m.

The basic integration scheme in the FEM involves evaluation of volume integrals. Hence the FEM has to choose, at the outset, a coordinate system of known symmetry, usually Cartesian. In addition, to facilitate evaluation of the volume integral, the elemental volume has to have a simple shape the volume of which can be expressed as a simple function of its dimensions. As a result, when the flow domain has a complex geometry with mixed symmetry, the FEM has to approximate the domain by using fundamental shapes such as triangles or squares, which may not always be easy. To some extent, this difficulty can be overcome by resorting to higher-order isoparametric elements.

In the case of IFDM, which basically evaluates surface fluxes and in which geometrical parameters are provided as input information, there is no restriction on choosing any basic elemental shape. Therefore arbitrarily shaped elements can be chosen judiciously not only to handle mixed symmetries (as was done in Figure 3) but also to fit complex boundaries with a small number of elements. A very desirable feature of the IFDM is that it can, in a simple way, handle complex boundaries and still retain a linear approximation for potential variation.

In the IFDM, care must be taken to design the mesh so that the lines joining nodal points coincide with the normals to the interfaces between the points. This restriction, as well as the requirement for providing geometrical parameters as input data, may require added effort in the design of networks for complex problems. To some extent, this effort can be minimized by developing auxiliary computer programs for mesh and input data generation. On the other hand, the design of the FEM mesh may be less restrictive, since the geometric parameters are generated implicitly in the volume integration. However, even in the FEM it may be necessary to have basic elements with some regularity of shape (e.g., to avoid obtuse-angled triangles) in order to avoid undesirable matrix properties that affect the efficiency of the solution process [*Neuman and Narasimhan,* 1976; *Narasimhan et al.,* 1976].

Certain apparent differences between IFDM and FEM arise mostly owing to the conventions and customary procedures that are followed. If we look at the conventional Galerkin form of the FEM equation (17), we note that the equation for nodal point m also contains the unknown time derivatives at the neighboring nodal points n. Hence the set of equations arising out of (17) would have to be solved as a set of simultaneous equations involving these unknowns. In other words, (17) cannot be solved explicitly, even for small time steps. On the other hand, the modified Galerkin equation in (18), which is similar to the IFDM (5) or (6), can be solved explicitly or implicitly as required.

In addition to their simplicity, an added advantage of IFDM equations is that local stability conditions are easier to define (7), and this has enabled the development of an optimal explicit-implicit procedure used in the program Trump. The IFDM has also been amenable to the development of a successful iterative scheme that has produced satisfactory results for a wide class of problems [*Edwards,* 1972; *Narasimhan,* 1975]. The result of using such a scheme is that IFDM is not constrained by the need for optimal numbering of nodal points, as is the case in some FEM schemes. Furthermore, a single computer program is able to handle one-, two- or three-dimensional problems, and the size of a problem does not necessarily depend on its dimensionality.

From the above discussion of IFDM and FEM we have seen that some of the differences are intrinsic in the methods used, while others are mainly a matter of convention. If suitable changes in convention could be made, it appears that one could combine the advantages of both methods and develop an improved numerical process.

As was discussed earlier, the modified Galerkin approach (18) is conceptually similar to (5) or (6) of the IFDM. An analysis of (18) has shown [*Neuman and Narasimhan,* 1976] that for this equation, not only is it possible to define a local stability criterion similar to (7) of the IFDM, but it is also possible to establish local convergence criteria for the numerical equation. Furthermore, (18) has also been found to be amenable to the iterative solution scheme of *Evans et al.* [1954] on which the explicit-implicit procedure of Trump is based. Therefore by incorporating (18) into the Trump algorithm we have been able to develop a new mixed explicit-implicit computer scheme for solving diffusion-type problems [*Neuman and Narasimhan,* 1976; *Narasimhan et al.,* 1976].

Conclusions

The theoretical basis for the integrated finite difference method reveals a rather simple but powerful numerical technique for solving groundwater flow problems. Examples have been provided to demonstrate that the IFDM as incorporated in Trump can handle two- or three-dimensional problems with ease.

A comparison of IFDM and FEM indicates that each of these integral methods has distinct advantages in handling certain classes of problems. The modified Galerkin form of the FEM is conceptually almost the same as the IFDM except for the difference in the procedure used in evaluating the gradient of ϕ. This suggests the possibility of developing a new FEM code that can incorporate the explicit-implicit iterative solution scheme in Trump and thus combine the advantages that are inherent in both IFDM and FEM.

Notation

$A_{m,n}$ area of interface between elements m and n in IFDM (L^2).
b fracture aperture (L).
c specific fluid capacity or specific storage ($1/L$).
$D_{m,n}$ distance between nodal points m and n in IFDM.
g flow rate per unit volume ($1/T$) or acceleration due to gravity in the fracture flow problem (L/T^2).
g_m flow rate per unit volume of element m ($1/T$).
K hydraulic conductivity (L/T).
$K_{m,n}$ mean hydraulic conductivity between elements m and n (L/T).
m subscript used to denote an element or a nodal point (1).
n subscript used to denote an element or a nodal point (1).
n unit outer normal to a surface (1).
Q flow rate (L^3/T)
r radial distance (L).
r_e radial distance to external boundary in fracture flow problem (L).
r_i radial distance to internal boundary in fracture flow problem (L).
S storage coefficient in Theis equation (1) or surface of integration.
t time (T).
T coefficient of transmissibility in Theis equation (L^2/T).
$U_{m,n}$ conductance between elements m and n (L^2/T).
V volume (L^3).

V_m volume of element m (L^3).
Δ^e area of triangular element e.
κ diffusivity (L^2/T).
λ weight given to the backward-differencing operation in the implicit scheme (1).
μ viscosity of fluid (M/LT).
ξ function to express the variation of potential over an element e in the FEM or the Galerkin weighting function (1).
ξ_m weighting function pertaining to nodal point m.
ρ density of fluid (M/L^3).
ϕ fluid potential or hydraulic head (L).

Acknowledgments. We would like to thank T. J. Lasseter and S. P. Neuman for many fruitful discussions during the preparation of this paper. We also appreciate the assistance of Katsuhiko Iwai in providing the solution for the fracture flow problem. This work was partially supported by the U.S. Energy Research and Development Administration.

REFERENCES

Carslaw, H. S., and J. C. Jaeger, *Conduction of Heat in Solids*, p. 261, Oxford at the Clarendon Press, London, 1959.

Cooley, R. L., A finite difference method for variably saturated porous media: Application to a single pumping well, *Water Resour. Res.*, *7*(6), 1607–1625, 1971.

Dusinberre, G. M., *Heat Transfer Calculations by Finite Differences*, International Textbooks, Scranton, Pa., 1961.

Edwards, A. L., *Trump: A Computer Program for Transient and Steady State Temperature Distributions in Multidimensional Systems*, National Technical Information Service, National Bureau of Standards, Springfield, Va., 1972.

Emery, A. F., and W. W. Carson, An evaluation of the use of the finite-element method in the computation of temperature, *J. Heat Transfer, 93*, 136–145, 1971.

Encyclopedia of Science and Technology, vol. 5, p. 45, McGraw-Hill, New York, 1960.

Evans, G. W., R. J. Brousseau, and R. Keirstead, Instability considerations for various difference equations derived from the diffusion equation, *Rep. UCRL-4476*, Lawrence Radiat. Lab., Livermore, Calif., 1954.

Felippa, C. A., Refined finite element analysis of linear and nonlinear two-dimensional structures, *Rep. SESM 66-22*, Dep. of Civil Eng., Univ. of Calif., Berkeley, 1966.

Gale, J. E., R. L. Taylor, P. A. Witherspoon, and M. S. Ayatollahi, Flow in rocks with deformable fractures, in *Finite Element Methods in Flow Problems*, edited by J. T. Oden et al., pp. 583–598, UAH Press, Huntsville, Ala., 1974.

Javandel, I., and P. A. Witherspoon, Application of the finite element method to transient flow in porous media, *Soc. Petrol. Eng. J.*, *8*(3), 241–250, 1968.

Louis, C., A study of groundwater flow in jointed rock and its influence on the stability of rock masses, *Rock Mech. Res. Rep. 10*, Imp. Coll., Univ. of London, London, 1969.

MacNeal, R. H., An asymmetric finite difference network, *Quart. Appl. Math., 2*, 295–310, 1953.

Narasimhan, T. N., A unified numerical model for saturated-unsaturated groundwater flow, Ph.D. thesis, Dep. of Civil Eng., Univ. of Calif., Berkeley, 1975.

Narasimhan, T. N., S. P. Neuman, and A. L. Edwards, Mixed explicit-implicit iterative finite element scheme for diffusion-type problems, 2, Solution strategy and examples, submitted to *Int. J. Numer. Methods Eng.*, 1976.

Neuman, S. P., Saturated-unsaturated seepage by finite elements, *J. Hydraul. Div. Amer. Soc. Civil Eng., 99*(HY 12), 2233–2250, 1973.

Neuman, S. P., Galerkin approach to saturated-unsaturated flow in porous media, in *Finite Elements in Fluids*, vol. 1, edited by R. H. Gallagher, chap. 10, John Wiley, New York, 1975.

Neuman, S. P., and T. N. Narasimhan, Mixed explicit-implicit iterative finite element scheme for diffusion-type problems, 1, Theory, submitted to *Int. J. Numer. Methods Eng.*, 1976.

O'Brien, G. G., M. A. Hyman, and S. Kaplan, A study of the numerical solution of partial differential equations, *J. Math. Phys., 29*, 223–251, 1951.

Pinder, G. F., and E. O. Frind, Application of Galerkin procedure to aquifer analysis, *Water Resour. Res.*, *8*(1), 108–120, 1972.

Romm, E. S., *Flow Phenomena in Fractured Rocks* (in Russian), Nedra, Moscow, 1966.

Sharp, J. C., and Y. N. T. Maini, Fundamental considerations on the hydraulic characteristics of joints in rock, in *Proceedings of Symposium on Percolation Through Fissured Rock*, pp. 1–15, Deutsche Gesellschaft für Erd-und-Grunabau, Essen, Germany, 1972.

Snow, D. T., A parallel plate model of fractured permeable media, Ph.D. thesis, Dep. of Civil Eng., Univ. of Calif., Berkeley, 1965.

Sokolnikoff, I. S., and R. M. Redheffer, *Mathematics of Physics and Modern Engineering*, McGraw-Hill, New York, 1966.

Theis, C. V., The relation between the lowering of the piezometric surface and the rate of duration and discharge of a well using groundwater storage, *Eos Trans. AGU, 16*, 519–524, 1935.

Todd, D. K., *Ground Water Hydrology*, John Wiley, New York, 1959.

Tyson, H. N., and E. M. Weber, Groundwater management for the nations future—Computer simulation of groundwater basins, *J. Hydraul. Div. Amer. Soc. Civil Eng., 90*(HY4), 59–77, 1964.

Wilson, C. R., and P. A. Witherspoon, Steady state flow in rigid networks of fractures, *Water Resour. Res., 10*(2), 328–335, 1974.

Wilson, E. L., The determination of temperatures within mass concrete structures, *SESM Rep. 68-17*, Dep. of Civil Eng., Univ. of Calif., Berkeley, 1968.

Winslow, A. M., Numerical solution of the quasilinear Poisson equation in a non-uniform triangle mesh, *J. Comput. Phys., 1*, 149–172, 1966.

Zienkiewicz, O. C., and C. J. Parekh, Transient field problems: Two-dimensional and three-dimensional analysis by isoparametric finite elements, *Int. J. Numer. Methods Eng., 2*, 61–71, 1970.

(Received May 5, 1975;
revised September 15, 1975;
accepted September 15, 1975.)